Spin-flip electron-energy-loss spectroscopy in itinerant-electron ferromagnets: Collective modes versus Stoner excitations

G. Vignale* and K. S. Singwi
Department of Physics and Astronomy, Northwestern University, Evanston, Illinois 60201
(Received 11 February 1985)

The energy-dependent spin-flip cross section due to exchange collisions of electrons with the spin-polarized electrons of an itinerant-electron ferromagnet is expressed in terms of a two-particle correlation function. For large momentum of the incident electron it is proportional to the transverse spin susceptibility and it is dominated by collective modes (magnons). For incident momentum comparable to the Fermi momentum of the ferromagnetic electrons a model calculation within the random-phase approximation shows that the cross section has a consistent contribution from spin-flip Stoner excitations even for very small momentum transfer. The Stoner part of the spectrum is found to be essentially free of Coulomb-interaction effects. Recent experimental results are discussed and compared with the predictions of the model. The possibility of measuring magnon dispersions by this technique is pointed out.

I. INTRODUCTION

Recent experiments by Hopster, Raue, and Clauberg[1] and by Kirschner, Rebenstorff, and Ibach[2] have demonstrated the possibility of studying the elementary excitations of an itinerant ferromagnet by means of a spin-polarized electron-energy-loss spectroscopy. Two complementary experiments have been performed. In the first one (Ref. 1) a beam of unpolarized electrons impinges on a ferromagnetic glass. The scattered beam is found to be polarized parallel to the direction of the polarization in the sample and the polarization, measured as a function of the energy loss, shows a peak around a value corresponding to the ferromagnetic exchange splitting. In the second experiment (Ref. 2) a beam of spin-polarized electrons impinges on a ferromagnetic crystal and the total scattered intensity for small momentum transfer is measured as a function of the energy loss. This measurement is performed with a definite initial polarization parallel or antiparallel to the polarization of the sample. The quantity of interest, the so-called asymmetry, i.e., the normalized difference between the scattered intensities for parallel and antiparallel initial polarization is generally negative and has, again, a peak around the value of the exchange splitting. The results of both experiments can be qualitatively understood in terms of spin-flipping exchange collisions. An example of such a process is shown in Fig. 1. An incident electron, which is polarized opposite to the polarization in the sample falls in a minority-spin state (↓) while a majority-spin electron (↑) is released from the system and emerges as the final electron. To an observer who only considers the initial and final states of the beam it appears as if a spin-flip event has taken place—although, in reality, no spin has been flipped. Moreover, a particle-hole pair carrying spin $S_z = -\hbar$ has been excited in the system. This simple picture is now sufficient to explain the results of Refs. 1 and 2. In the first case it is clear that if the incident electron has spin ↓, an exchange collision of the kind described above can easily occur, but if the incident electron has spin ↑ this becomes very unlikely, since the majority-spin band has very few empty states to accommodate the incoming electron. As a consequence, the final beam is expected to contain more spin-↑ electrons (from exchange collisions) than spin-↓ electrons. This gives a polarization parallel to the polarization of the sample. Similarly, in the second case, the total scattered intensity for incident spin-↓ electrons will be larger than for incident spin-↑ electrons, due to the contribution of exchange collisions to the former. This results in a negative asymmetry. In both cases, the spin-flip process is accompanied by the creation of a particle-hole pair across the Stoner gap having a characteristic energy in the neighborhood of the exchange splitting. This explains the presence of a peak in the energy-loss spectra around the value of the exchange splitting.

It is characteristic of the above discussion that it does not require anything more complicated than the bare Coulomb interaction between the external electron and

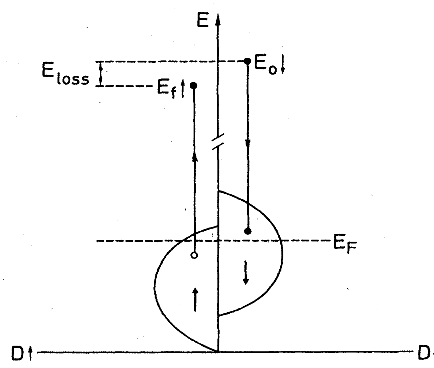

FIG. 1. Schematic density-of-states diagram of a spin-flip exchange collision. The incoming electron ($E_{0\downarrow}$) falls in the minority band. An electron from the majority band emerges as the outgoing one ($E_{f\uparrow}$).

one of the internal electrons plus the phase-space restrictions imposed by the exclusion principle. The internal electrons, however, are also interacting via the Coulomb force and must therefore display collective behavior: in particular, besides the simple Stoner-pair excitations, they can sustain transverse spin oscillations (magnons) and multipair excitations. A complete theory of the exchange-collision process should account for the existence of such excitations.

In this paper we shall be mainly concerned with the question of the relative weight of the collective (magnon) and single-pair (Stoner) contributions to the spin-flip inelastic cross section.[3] In the case of neutron scattering, another technique which probes the magnetic excitations of a ferromagnet, the inelastic cross section at low temperature and small momentum transfer is dominated by magnons.[4] The small Stoner contribution as calculated from simple models of the transverse spin susceptibility also shows an interesting interaction effect in that the position of its peak is shifted to lower frequency relative to the noninteracting Stoner peak. Returning to the electron-energy-loss experiments we may wonder whether the situation with regards to these spin-carrying excitations is the same as in neutron scattering experiments or there are some differences due to the peculiar character of the exchange process. In order to answer this question we introduce the general formalism required to treat the exchange collisions in a many-body system. The differential cross section (in Born approximation) for a spin-flip collision of the kind described above can be expressed as the imaginary part of a retarded response function $\chi_\sigma(\mathbf{p}_0,\mathbf{q},E)$, where σ and $\mathbf{p}_0$ are the spin and momentum of the incident electron, $\mathbf{q}$ and E are the momentum and energy transfers. In the limit of very large initial momentum χ_σ becomes proportional to the transverse spin-spin response function, the constant of proportionality being the square of the Fourier-transformed Coulomb interaction $V^2(p_0)$. Thus, in this limit, the electron-energy-loss cross section is expected to have the same shape as the neutron cross section, differing from it only for the absolute magnitude which decreases in the former case with the square of the primary energy. For smaller values of the incident momentum we can evaluate χ_0 within the random-phase approximation (RPA) of Izuyama, Kim, and Kubo[4] (IKK) using, as those authors, a model Hamiltonian with a repulsive δ-function interaction of strength U between electrons of antiparallel spin. We find the following: (i) The relative contribution of Stoner pairs to the total cross section is considerably larger than in the case of neutron scattering. In particular, it does not tend to zero for $q \rightarrow 0$ and becomes larger than the magnon contribution for sufficiently small p_0. (ii) The shape of the Stoner excitation spectrum is similar to that of the corresponding noninteracting spectrum: in particular, its peak does not show any tendency to move toward smaller energy. Thus, we can conclude that the electronic spin-flip cross section is much less influenced by many-body effects than the corresponding neutron cross section. Nevertheless, an important many-body effect is present, since the incoming electron can, in the course of the exchange process, excite a magnon. This effect gives rise to a low-energy peak in the cross section which, we suggest, should be observable in an experiment with sufficiently large momentum transfer.[5]

Using our model evaluation of χ_σ we have also attempted to reproduce the shapes of the experimental curves of Refs. 1 and 2 for the polarization and the asymmetry, respectively. In the first case the scattering is from a glassy sample which diffuses the electrons at all angles. This experiment is clearly not q resolved. Integrating the model cross section over a reasonable range of momentum transfers we find a curve which is in qualitative agreement with the experimental one, having a peak at the value of the exchange splitting and decreasing at higher values of the energy loss. The most relevant discrepancy is the presence of a magnon peak at low energy, which is absent in the experimental curve, possibly for lack of resolution. In the second case the experiment is q resolved (only excitations with $q \sim 0$ are probed) and we find that it is not possible, within our model, to reproduce the broad distribution of the asymmetry around the exchange splitting. As noted by the authors of Ref. 2 this width can be interpreted as a measure of the nonuniformity of the exchange splitting over the Brillouin zone. Our model assumes rigidly split bands and therefore gives a much narrower distribution of asymmetry for $q \sim 0$. It is interesting to notice that by allowing a certain amount of nonuniformity in the exchange splitting in the analysis of the first experiment one would also find a broader curve in better agreement with the experimental curve.

This paper is organized as follows: In Sec. II we introduce the formalism appropriate to calculate the inelastic cross section for exchange collisions. In Sec. III we present a model evaluation, within the RPA, of the response function which gives the inelastic cross section. In Sec. IV we discuss the many-body effects in our model, compare the electron cross section with the neutron cross section for the same kind of excitations and discuss the relation of our results to the experiments of Refs. 1 and 2.

II. FORMALISM

In this section we introduce the formalism appropriate to calculate the energy-loss cross section for exchange collisions. Let $\phi_i(\mathbf{r}_1,\sigma_1;\mathbf{r}_2,\sigma_2;\ldots;\mathbf{r}_N,\sigma_N)$ and $\phi_f(\mathbf{r}_1,\sigma_1;\mathbf{r}_2,\sigma_2;\ldots;\mathbf{r}_N,\sigma_N)$ represent the wave functions of the N-electron system before and after the scattering. These are functions of the coordinates and the spins ($\mathbf{r}$'s and σ's) of all the electrons and must be antisymmetric with respect to the interchange of any two electrons: $(\mathbf{r}_i,\sigma_i) \longleftrightarrow (\mathbf{r}_j,\sigma_j)$, $i \neq j$. The total wave function of the N-electron system plus the incident electron before the scattering can be taken as

$$\psi_i(\mathbf{r},\sigma;\mathbf{r}_1,\sigma_1;\mathbf{r}_2,\sigma_2;\ldots;\mathbf{r}_N,\sigma_N) = \phi_i(\mathbf{r}_1,\sigma_1;\mathbf{r}_2,\sigma_2;\ldots;\mathbf{r}_N,\sigma_N)e^{i\mathbf{p}_0\cdot\mathbf{r}}\chi_i(\sigma) , \qquad (1)$$

where $\mathbf{r}$ and σ refer to the incident electron, whose momentum is $\mathbf{p}_0$ and whose spin state is described by the wave function $\chi_i(\sigma)$. Equation (1) is clearly not antisymmetric under interchange of the "external" electron with an "internal" one and, in fact, need not be so, since the external electron is definitely distinguishable, at this stage, from any internal electron. A complete antisymmetrization of the wave function is, however, essential to describe the state of the system *after* the collision, since, in this case, it is not possible to say whether the emerging electron is the same one which left the electron source or a "new" one emitted from the metal. Thus, we write

$$\psi_f(\mathbf{r},\sigma;\mathbf{r}_1,\sigma_1;\mathbf{r}_2,\sigma_2;\ldots;\mathbf{r}_N,\sigma_N)=\phi_f(\mathbf{r}_1,\sigma_1;\mathbf{r}_2,\sigma_2;\ldots;\mathbf{r}_N,\sigma_N)e^{i\mathbf{p}_f\cdot\mathbf{r}}\chi_f(\sigma) - \sum_{i=1}^{N}\phi_f^{(i)}(\mathbf{r}_1,\sigma_1;\ldots;\mathbf{r}_{i-1},\sigma_{i-1};\mathbf{r},\sigma;\mathbf{r}_{i+1},\sigma_{i+1};\ldots;\mathbf{r}_N,\sigma_N)e^{i\mathbf{p}_f\cdot\mathbf{r}_i}\chi_f(\sigma_i)\ , \quad (2)$$

where $\mathbf{p}_f$ and χ_f are the momentum and the spin wave function of the emerging electron and $\phi_f^{(i)}$ denotes the function obtained from ϕ_f after replacing the arguments $\mathbf{r}_i,\sigma_i$ by $\mathbf{r},\sigma$. It is easy to verify that the wave function of Eq. (2) is totally antisymmetric under interchange of two electrons. Its second term, which is normally disregarded in the theory of high-energy scattering as a minor correction to the main direct term, is now exactly the one which accounts for the possibility of spin flip.

The interaction between the incident electron and the system is taken to be a simple longitudinal Coulomb interaction:

$$H_I=\sum_{i=1}^{N}v(|\mathbf{r}-\mathbf{r}_i|)\ ,\qquad v(r)=e^2/r\ . \quad (3)$$

Within the first Born approximation the scattering amplitude is given by the matrix element of H_I between the initial and final states represented by the wave functions (1) and (2).

The matrix element of H_I between the initial wave function ψ_i and the first term of the final wave function ψ_f gives the direct scattering amplitude:

$$A^d_{p_0,\sigma_0\to p_f,\sigma_f}=\left[\sum_\sigma \chi_i(\sigma)\chi_f^*(\sigma)\right]V_q\sum_{\sigma_1,\sigma_2,\ldots,\sigma_N}\int\prod_{k=1}^{N}d\mathbf{r}_k\,\phi_f^*(\mathbf{r}_1,\sigma_1;\mathbf{r}_2,\sigma_2;\ldots;\mathbf{r}_N,\sigma_N)\rho_q\phi_i(\mathbf{r}_1,\sigma_1;\mathbf{r}_2,\sigma_2;\ldots;\mathbf{r}_N,\sigma_N)\ , \quad (4)$$

where $\mathbf{q}=\mathbf{p}_0-\mathbf{p}_f$ is the momentum transfer, $V_q=4\pi e^2/q^2$ is the Fourier transform of the Coulomb potential, and

$$\rho_q=\sum_{i=1}^{N}e^{i\mathbf{q}\cdot\mathbf{r}_i}$$

is the usual density-fluctuation operator. If χ_i and χ_f are eigenstates of the z component of the spin, namely $\chi_i(\sigma)=\delta_{\sigma,\sigma_0}$ and $\chi_f(\sigma)=\delta_{\sigma,\sigma_f}$, the sum over σ in Eq. (4) gives a factor $\delta_{\sigma_0,\sigma_f}$. Thus, direct scattering preserves the spin of the incident electron, which is not surprising for a spin-independent interaction. Next we consider the effect of the remaining N terms in ψ_f. They give an exchange scattering amplitude equal to

$$A^x_{p_0,\sigma_0\to p_f,\sigma_f}=-\sum_{i=1}^{N}\sum_{j=1}^{N}\sum_{\sigma_1,\sigma_2,\ldots,\sigma_N,\sigma}\Bigg[\chi_i(\sigma)\chi_f^*(\sigma_i)\int d\mathbf{r}\prod_{K=1}^{N}d\mathbf{r}_K e^{i\mathbf{p}_0\cdot\mathbf{r}}e^{-i\mathbf{p}_f\cdot\mathbf{r}_i}\phi_i(\mathbf{r}_1,\sigma_1;\mathbf{r}_2,\sigma_2;\ldots;\mathbf{r}_N,\sigma_N) \times\phi_f^{*(i)}(\mathbf{r}_1,\sigma_1;\ldots;\mathbf{r}_{i-1},\sigma_{i-1};\mathbf{r},\sigma;\mathbf{r}_{i+1},\sigma_{i+1};\ldots;\mathbf{r}_N,\sigma_N) \times v(|\mathbf{r}-\mathbf{r}_j|)\Bigg]\ . \quad (5)$$

The terms with $i=j$ on the right-hand side of Eq. (5) can be written as

$$-\frac{1}{N}\sum_{i=1}^{N}\int d\mathbf{r}\,d\mathbf{r}_i\,e^{i\mathbf{p}_0\cdot\mathbf{r}}e^{-i\mathbf{p}_f\cdot\mathbf{r}_i}v(|\mathbf{r}-\mathbf{r}_i|) \times\langle f\,|\,\psi^\dagger_{\sigma_0}(\mathbf{r})\psi_{\sigma_f}(\mathbf{r}_i)\,|\,i\rangle\ , \quad (6)$$

where $\psi_0(\mathbf{r})$ is the usual field operator which destroys an electron of spin σ at position $\mathbf{r}$ in the N-electron system. In order to derive Eq. (6) we have taken for χ_i and χ_f eigenstates of σ_z with eigenvalues σ_0,σ_f and we have used the well-known expression for the simultaneous eigenstates of positions and spins of the system:

$$|\,\mathbf{r}_1,\sigma_1;\mathbf{r}_2,\sigma_2;\ldots;\mathbf{r}_N,\sigma_N\rangle =\frac{1}{(N!)^{1/2}}\psi^\dagger_{\sigma_1}(\mathbf{r}_1)\psi^\dagger_{\sigma_2}(\mathbf{r}_2)\cdots\psi^\dagger_{\sigma_N}(\mathbf{r}_N)\,|\text{ vacuum}\rangle\ . \quad (7)$$

The connection between the abstract state $|\,S\rangle$ and its wave function ϕ_s is naturally

$$\phi_s(\mathbf{r}_1,\sigma_1;\mathbf{r}_2,\sigma_2;\ldots;\mathbf{r}_N,\sigma_N) =\langle\mathbf{r}_1,\sigma_1;\mathbf{r}_2,\sigma_2;\ldots;\mathbf{r}_N,\sigma_N\,|\,S\rangle\ . \quad (8)$$

A similar treatment can be applied to the terms with $i\neq j$ in Eq. (5) with the result

$$-\frac{1}{N(N-1)}\sum_{\substack{i,j,\sigma_j\\ i\neq j}}\int d\mathbf{r}\,d\mathbf{r}_i\,d\mathbf{r}_j\,e^{i\mathbf{p}_0\cdot\mathbf{r}}e^{-i\mathbf{p}_f\cdot\mathbf{r}_i}v(|\mathbf{r}-\mathbf{r}_j|)\langle f|\psi^\dagger_{\sigma_0}(\mathbf{r})\psi^\dagger_{\sigma_j}(\mathbf{r}_j)\psi_{\sigma_j}(\mathbf{r}_j)\psi_{\sigma_f}(\mathbf{r}_i)|i\rangle\ . \tag{9}$$

The integral over $\mathbf{r}_i$ in this expression gives the annihilation operator for the state of the final electron acting on the initial state of the system. This is essentially zero, since the state of the emerging electron is well above the Fermi energy of the system. Thus, the last line of Eq. (6) gives the exchange-scattering amplitude in Born approximation. From now on we shall only concentrate on the spin-flip processes in which the direct term [Eq. (4)] is absent. We introduce the operator

$$\rho^\dagger_{\sigma_0\sigma_f}(\mathbf{p}_0,\mathbf{q})=\frac{1}{N}\sum_{i=1}^{N}\int d\mathbf{r}\,d\mathbf{r}_i\,e^{i\mathbf{p}_0\cdot\mathbf{r}}e^{-i\mathbf{p}_f\cdot\mathbf{r}_i}\times v(|\mathbf{r}-\mathbf{r}_i|)\psi^\dagger_{\sigma_0}(\mathbf{r})\psi_{\sigma_f}(\mathbf{r}_i) \tag{10}$$

($\mathbf{p}_f=\mathbf{p}_0-\mathbf{q}$). The double-differential cross section for an exchange collision with spin flip ($\sigma_f=-\sigma_0$) is obtained by summing the scattering probability over the final states and averaging over the initial states. This gives

$$\frac{d^2\sigma}{dE\,d\Omega}=\frac{m^2}{4\pi^2\hbar^4}\frac{p_f}{p_0}\frac{1}{Z}\sum_{i,f}e^{-\beta E_i}|\langle f|\rho^\dagger_{\sigma_0,-\sigma_0}(\mathbf{p}_0,\mathbf{q})|i\rangle|^2\times\delta(E-E_f+E_i)\ , \tag{11}$$

where $\beta=1/k_BT$, E is the energy loss, Ω is the solid angle, Z is the canonical partition function, and E_f and E_i are the exact energies of the states $|f\rangle$ and $|i\rangle$. A more convenient way of writing Eq. (11) is

$$\frac{d^2\sigma}{dE\,d\Omega}=-\frac{m^2}{4\pi^2\hbar^4}\frac{p_f}{p_0}\frac{1}{\pi}\frac{\mathrm{Im}\chi_{\sigma_0}(\mathbf{p}_0,\mathbf{q},E)}{1-e^{-\beta E}}\ , \tag{12}$$

where $\chi_{\sigma_0}(\mathbf{p}_0,\mathbf{q},E)$ is the linear-response function:

$$\chi_{\sigma_0}(\mathbf{p}_0,\mathbf{q},E)=\frac{1}{Z}\sum_{i,f}e^{-\beta E_i}\left[\frac{|\langle f|\rho^\dagger_{\sigma_0,-\sigma_0}(\mathbf{p}_0,\mathbf{q})|i\rangle|^2}{E-E_f+E_i+i0}-\frac{|\langle f|\rho_{\sigma_0,-\sigma_0}(\mathbf{p}_0,\mathbf{q})|i\rangle|^2}{E+E_f-E_i+i0}\right]\ , \tag{13}$$

which is also equal to the analytic continuation ($\omega\to E+i\eta$) of the time-ordered autocorrelation spectrum:

$$\chi^T_{\sigma_0}(\mathbf{p}_0,\mathbf{q},i\omega_n)=-\int_0^\beta d\tau\,e^{i\omega_n\tau}\langle T_\tau[\rho_{\sigma_0,-\sigma_0}(\mathbf{p}_0,\mathbf{q},\tau)\times\rho^\dagger_{\sigma_0,-\sigma_0}(\mathbf{p}_0,\mathbf{q})]\rangle\ , \tag{14}$$

where $\omega_n=2\pi n/\beta$ is a bosonic Matsubara frequency and $\langle\cdots\rangle$ denotes the thermal and quantum average. Equations (10)—(14) constitute a complete set of equations for the calculation of the spin-flip cross section from a general inhomogeneous electron system. Equation (14) is amenable to a systematic expansion in Feynman diagrams.

In the rest of this paper we shall only consider the very simple case of exchange scattering from a homogeneous spin-polarized electron gas. Such a model is probably not an unreasonable idealization for the behavior of the electrons in a very narrow d band in an itinerant ferromagnet. The field operator $\psi_0(\mathbf{r})$ can be expanded in this case as

$$\psi_\sigma(\mathbf{r})=\frac{1}{V^{1/2}}\sum_{\mathbf{k}}e^{i\mathbf{k}\cdot\mathbf{r}}a_{\mathbf{k},\sigma}\ . \tag{15}$$

Inserting this expansion in Eq. (10) and performing the various integrations, it is straightforward to show that

$$\rho^\dagger_{\sigma_0,\sigma_f}(\mathbf{p}_0,\mathbf{q})=\sum_{\mathbf{k}}V(\mathbf{p}_0-\mathbf{k}-\mathbf{q}/2)a^\dagger_{\mathbf{k}+\mathbf{q}/2,\sigma_0}a_{\mathbf{k}-\mathbf{q}/2,\sigma_f}\ . \tag{16}$$

This expression could have been written at once by examining the exchange-collision diagram of an electron on a system of noninteracting electrons. Such a diagram is shown in Fig. 2. As a result of the collision the system remains with an electron excited in $\mathbf{k}+\mathbf{q}/2,\sigma_0$ (above the Fermi surface) and a hole left in $\mathbf{k}-\mathbf{q}/2,\sigma_f$. This particle-hole state is created by the two operators in Eq. (16). The matrix element for this process is exactly $V(\mathbf{p}_0-\mathbf{k}-\mathbf{q}/2)$.

III. EVALUATION OF THE SPIN-FLIP CROSS SECTION IN THE RPA

In order to evaluate the response function $\chi_\sigma(\mathbf{p}_0,\mathbf{q},E)$ we follow the standard RPA procedure, already used by Izuyama, Kim, and Kubo[4] and many others to calculate the spin-spin correlation functions of a spin-polarized

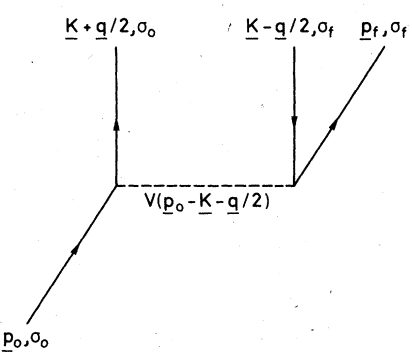

FIG. 2. The simplest contribution to the spin-flip scattering amplitude. Interactions between the "internal" electrons are not included.

electron gas. First of all, we assume a simplified Hamiltonian for the system:

$$H=\sum_{\mathbf{p},\sigma}\varepsilon_{\mathbf{p}}a^{\dagger}_{\mathbf{p},\sigma}a_{\mathbf{p},\sigma}+U\sum_{\mathbf{p},\mathbf{p}',\mathbf{q}}a^{\dagger}_{\mathbf{p}+\mathbf{q},\uparrow}a_{\mathbf{p},\uparrow}a^{\dagger}_{\mathbf{p}'-\mathbf{q},\downarrow}a_{\mathbf{p}',\downarrow}\ , \tag{17}$$

where $\varepsilon_p=\hbar^2p^2/2m_B-\mu$ (μ is the chemical potential and m_B is the effective mass of the band). This is a version of the Hubbard model for band ferromagnetism, which is believed to be appropriate to describe the main features of electron correlations in narrow energy bands, leading to itinerant-electron magnetism.

As a second step we write the equation of motion for the operator $\theta_\sigma(\mathbf{p}_0,\mathbf{k},\mathbf{q})$, defined as

$$\theta_\sigma(\mathbf{p}_0,\mathbf{k},\mathbf{q})=V(\mathbf{p}_0-\mathbf{k}-\mathbf{q}/2)a^{\dagger}_{\mathbf{k}-\mathbf{q}/2,-\sigma}a_{\mathbf{k}+\mathbf{q}/2,\sigma}\ . \tag{18}$$

It is a matter of simple algebraic manipulations to prove that

$$\begin{aligned}\frac{\partial}{\partial\tau}\theta_\sigma(\mathbf{p}_0,\mathbf{k},\mathbf{q})&=-[\theta_\sigma(\mathbf{p}_0,\mathbf{k},\mathbf{q}),H]\\&=-(\varepsilon_{\mathbf{k}+\mathbf{q}/2}-\varepsilon_{\mathbf{k}-\mathbf{q}/2})\theta_\sigma(\mathbf{p}_0,\mathbf{k},\mathbf{q})-UV(\mathbf{p}_0-\mathbf{k}-\mathbf{q}/2)\\&\quad\times\sum_{\mathbf{p},\mathbf{q}'}(a^{\dagger}_{\mathbf{k}-\mathbf{q}/2,-\sigma}a^{\dagger}_{\mathbf{p}+\mathbf{q}',-\sigma}a_{\mathbf{p},-\sigma}a_{\mathbf{k}+\mathbf{q}'+\mathbf{q}/2,\sigma}-a^{\dagger}_{\mathbf{k}-\mathbf{q}/2+\mathbf{q}',-\sigma}a^{\dagger}_{\mathbf{p}-\mathbf{q}',\sigma}a_{\mathbf{p},\sigma}a_{\mathbf{k}+\mathbf{q}/2,\sigma})\ .\end{aligned} \tag{19}$$

The random-phase approximation consists of replacing the pairs of operators $a^{\dagger}a$ in the last term of Eq. (19) by their average values $\langle a^{\dagger}a\rangle$ in all possible ways. Thus one finds

$$\begin{aligned}\frac{\partial}{\partial\tau}\theta_\sigma(\mathbf{p}_0,\mathbf{k},\mathbf{q})=&-(\varepsilon_{\mathbf{k}+\mathbf{q}/2,\sigma}-\varepsilon_{\mathbf{k}-\mathbf{q}/2,-\sigma})\theta_\sigma(\mathbf{p}_0,\mathbf{k},\mathbf{q})\\&+(n_{\mathbf{k}-\mathbf{q}/2,-\sigma}-n_{\mathbf{k}+\mathbf{q}/2,\sigma})UV(\mathbf{p}_0-\mathbf{k}-\mathbf{q}/2)\sum_{\mathbf{q}'}a^{\dagger}_{\mathbf{k}-\mathbf{q}/2+\mathbf{q}',-\sigma}a_{\mathbf{k}+\mathbf{q}/2+\mathbf{q}',\sigma}\ ,\end{aligned} \tag{20}$$

where

$$\varepsilon_{\mathbf{k},\sigma}\equiv\varepsilon_k+Un_{-\sigma} \tag{21}$$

is the single-particle energy for spin σ. In this approximation, therefore, there is a rigid splitting between the spin-up (majority) and spin-down (minority) bands, the magnitude of the splitting being equal to $U(n_\uparrow-n_\downarrow)$.

From Eq. (20) one can easily derive the equation of motion for the time-ordered autocorrelation function,

$$\chi^{(2)}_{\mathbf{k},\mathbf{k}',\sigma}(\tau)=\langle T_\tau[\theta_\sigma(\mathbf{p}_0,\mathbf{k},\mathbf{q};\tau)\theta^{\dagger}_\sigma(\mathbf{p}_0,\mathbf{k}',\mathbf{q})]\rangle\ . \tag{22}$$

This equation is

$$\begin{aligned}\frac{\partial}{\partial\tau}\chi^{(2)}_{\mathbf{k},\mathbf{k}',\sigma}(\tau)=&\,\delta(\tau)\delta_{\mathbf{k},\mathbf{k}'}(n_{\mathbf{k}-\mathbf{q}/2,-\sigma}-n_{\mathbf{k}+\mathbf{q}/2,\sigma})[V(\mathbf{p}_0-\mathbf{k}-\mathbf{q}/2)]^2-(\varepsilon_{\mathbf{k}+\mathbf{q}/2,\sigma}-\varepsilon_{\mathbf{k}-\mathbf{q}/2,-\sigma})\chi^{(2)}_{\mathbf{k},\mathbf{k}',\sigma}(\tau)\\&+V(\mathbf{p}_0-\mathbf{k}-\mathbf{q}/2)U(n_{\mathbf{k}-\mathbf{q}/2,-\sigma}-n_{\mathbf{k}+\mathbf{q}/2,\sigma})\sum_{\mathbf{q}'}\langle T_\tau[a^{\dagger}_{\mathbf{q}'-\mathbf{q}/2,-\sigma}(\tau)a_{\mathbf{q}'+\mathbf{q}/2,\sigma}(\tau)\theta^{\dagger}_\sigma(\mathbf{p}_0,\mathbf{k}',\mathbf{q})]\rangle\ .\end{aligned} \tag{23}$$

Equation (23) now involves the correlation function

$$\chi^{(1)}_{\mathbf{q}',\mathbf{k}',\sigma}(\tau)=\langle T_\tau[a^{\dagger}_{\mathbf{q}'-\mathbf{q}/2,-\sigma}(\tau)a_{\mathbf{q}'+\mathbf{q}/2,\sigma}(\tau)\theta^{\dagger}_\sigma(\mathbf{p}_0,\mathbf{k}',\mathbf{q})]\rangle\ . \tag{24}$$

Taking the Fourier transform and summing over $\mathbf{k}$ and $\mathbf{k}'$, one finds

$$\begin{aligned}\chi^{T}_\sigma(\mathbf{p}_0,\mathbf{q},i\omega_n)=-\sum_{\mathbf{k},\mathbf{k}'}\chi^{(2)}_{\mathbf{k},\mathbf{k}'\sigma}(i\omega_n)=&\sum_{\mathbf{k}}\frac{n_{\mathbf{k}-\mathbf{q}/2,-\sigma}-n_{\mathbf{k}+\mathbf{q}/2,\sigma}}{i\omega_n-\varepsilon_{\mathbf{k}+\mathbf{q}/2,\sigma}+\varepsilon_{\mathbf{k}-\mathbf{q}/2,-\sigma}}V(\mathbf{p}_0-\mathbf{k}-\mathbf{q}/2)\\&\times\left[V(\mathbf{p}_0-\mathbf{k}-\mathbf{q}/2)+U\sum_{\mathbf{k}',\mathbf{q}'}\chi^{(1)}_{\mathbf{q}',\mathbf{k}'\sigma'}(i\omega_n)\right]\ .\end{aligned} \tag{25}$$

It remains to calculate $\sum_{\mathbf{k}',\mathbf{q}'}\chi^{(1)}_{\mathbf{q}',\mathbf{k}',\sigma}(i\omega)$. The equation of motion for $\chi^{(1)}_{\mathbf{k},\mathbf{k}',\sigma}(\tau)$ is very similar to Eq. (23), with the only difference that a factor $v(\mathbf{p}_0-\mathbf{k}-\mathbf{q}/2)$ is removed from the right-hand side:

$$\begin{aligned}\frac{\partial}{\partial\tau}\chi^{(1)}_{\mathbf{k},\mathbf{k}',\sigma}(\tau)=&\,\delta(\tau)V(\mathbf{p}_0-\mathbf{k}-\mathbf{q}/2)(n_{\mathbf{k}-\mathbf{q}/2,-\sigma}-n_{\mathbf{k}+\mathbf{q}/2,\sigma})\\&-(\varepsilon_{\mathbf{k}+\mathbf{q}/2,\sigma}-\varepsilon_{\mathbf{k}-\mathbf{q}/2,-\sigma})\chi^{(1)}_{\mathbf{k},\mathbf{k}',\sigma}(\tau)+U(n_{\mathbf{k}-\mathbf{q}/2,-\sigma}-n_{\mathbf{k}+\mathbf{q}/2,\sigma})\sum_{\mathbf{q}'}\chi^{(1)}_{\mathbf{q}',\mathbf{k}',\sigma}\ .\end{aligned}$$

This equation can be Fourier-transformed and summed over $\mathbf{k}$ and $\mathbf{k}'$ to find:

$$\sum_{\mathbf{k},\mathbf{k}'} \chi^{(1)}_{\mathbf{k},\mathbf{k}',\sigma}(i\omega_n) = -\frac{\chi^{(1)}_\sigma(\mathbf{p}_0,\mathbf{q},i\omega_n)}{1+U\chi^{(0)}_\sigma(\mathbf{q},i\omega_n)} , \tag{26}$$

where we have introduced the notation

$$\chi^{(i)}_\sigma(\mathbf{p}_0,\mathbf{q},i\omega_n) = \sum_{\mathbf{k}} \frac{n_{\mathbf{k}-\mathbf{q}/2,-\sigma} - n_{\mathbf{k}+\mathbf{q}/2,\sigma}}{i\omega_n + \varepsilon_{\mathbf{k}-\mathbf{q}/2,-\sigma} - \varepsilon_{\mathbf{k}+\mathbf{q}/2,\sigma}} \times [v(\mathbf{p}_0-\mathbf{k}-\mathbf{q}/2)]^i . \tag{27}$$

Notice that $\chi^{(0)}_\sigma(q,i\omega)$ is the transverse spin susceptibility of the homogeneous noninteracting electron gas and it is obviously independent of $\mathbf{p}_0$. Combining Eqs. (25)–(27) we arrive at the final formula for the RPA response function for spin-flip exchange collisions:

$$\chi_\sigma(\mathbf{p}_0,\mathbf{q},i\omega_n) = \chi^{(2)}_\sigma(\mathbf{p}_0,\mathbf{q},i\omega_n) - \frac{U[\chi^{(1)}_\sigma(\mathbf{p}_0,\mathbf{q},i\omega_n)]^2}{1+U\chi^{(0)}_\sigma(q,i\omega_n)} . \tag{28}$$

The first term on the right-hand side of this expression represents the free-electron contributions and the second one the many-body corrections. In the limit of very large momentum of the incident electron we can make the approximation

$$v(\mathbf{p}_0-\mathbf{k}-\mathbf{q}/2) \cong v(p_0) ,$$

and $\chi(\mathbf{p}_0,\mathbf{q},i\omega)$ reduces to

$$V^2(p_0)\frac{\chi^0(q,i\omega)}{1+U\chi^0(q,i\omega)} , \tag{29}$$

which is proportional to the RPA expression for the transverse spin susceptibility of the interacting electron gas. Equation (29) was taken by IKK as the staring point for the theory of neutron scattering from ferromagnetic d electrons. Thus, we see that, apart from the strong dependence on primary energy implied by the factor $v^2(p_0)$, the spin-flip cross section in electron scattering reduces to the spin-flip cross section in neutron scattering at sufficiently high energy. In particular, the excitation spectrum for small momentum transfer should be dominated in this limit by collective oscillations (magnons). As we shall see in the following section, this is no longer the case when the momentum of the incident electron becomes comparable to the Fermi momentum.

IV. CALCULATIONS AND DISCUSSION

We have considered a very simple model consisting of two rigidly split free-electron bands, the lower one for the majority-spin orientation and the upper one for the minority-spin orientation (see Fig. 3). The amount of splitting is taken to be equal to the Fermi energy. At $T=0$, therefore, only the majority-spin band is occupied and the interaction parameter U is equal to E_F/n, where n is the density of d electrons. The two bands are very narrow, having an effective mass m_B several times larger than the bare electron mass. In this way we hope to have

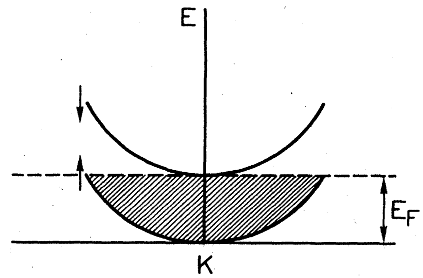

FIG. 3. Model of a uniformly polarized electron gas. The spin-↑ and spin-↓ bands are parabolic with effective mass m_B and split by a constant amount equal to the Fermi energy.

modeled the main features of the d-electron subsystem in an itinerant-electron ferromagnet, in particular, the strong peaks in the density of states of spin-↑ and spin-↓ electrons just below and above the Fermi energy,[6] but, of course, all the effects associated with the details of the band structure have been lost.

We propose to study the relative importance of collective modes (magnons) and Stoner pair excitations in the spin-flip cross section. We use Eq. (28) of the preceding section with the definitions given in Eq. (27) and concentrate on the relevant case $\sigma=\downarrow$, i.e., of an incident electron with spin antiparallel to the polarization. The noninteracting transverse susceptibility $\chi_{0\downarrow}(q,E)$ is readily calculated for the model at $T=0$ and it is

$$\chi_{0\downarrow}(\mathbf{q},E) = \frac{m}{8\pi^2\hbar^2}\frac{1}{\mathbf{q}}\psi(k_F, m_B(E-E_F)/\hbar^2 q - \tfrac{1}{2}\mathbf{q}) , \tag{30}$$

where

$$\psi(K,E) = 2KE - (E^2-K^2)\,\mathrm{Ln}\left[\frac{E+K}{E-K}\right] , \tag{31}$$

k_F is the band Fermi momentum for spin-↑ electrons and $\mathrm{Ln}z = \ln z + i\arg(z)$ is the complex logarithm. The imaginary part of $\chi^{(1)}_\downarrow(\mathbf{p}_0,\mathbf{q},E)$ and $\chi^{(2)}_\downarrow(\mathbf{p}_0,\mathbf{q},E)$ can also be evaluated analytically at $T=0$ and their expressions are given in the Appendix. From the imaginary parts the real parts of these functions can then be evaluated numerically using the Kramers-Kronig dispersion relations.

The general features of the excitation spectrum $\mathrm{Im}\chi_\downarrow(\mathbf{p}_0,\mathbf{q},E)$ in the $E,\mathbf{q}$ plane are the same as those of the transverse spin-fluctuation excitation spectrum, namely there is a line of singularity (magnons) at low energy corresponding to the zeros of the denominator in Eq. (28) and a continuous distribution of Stoner-pair excitations for $E_-(q) < E < E_+(q)$, where the kinematic boundaries $E_\pm(q)$ are given by the formula

$$E_\pm(q) = E_F \pm \hbar^2 q k_F/m_B + \hbar^2 q^2/2m_B . \tag{32}$$

For $q\to 0$ the energy of a Stoner pair tends to $E_\pm(0)=E_F$, which is the energy required to flip a spin without momentum transfer. From the small q expansion of $\chi^0_\downarrow(q,E)$,

$$\chi^0_\downarrow(q,E) \sim \frac{n}{E-E_F} + \frac{n\hbar^2 q^2/2m_B}{(E-E_F)^2} + \frac{1}{5}\frac{\hbar^2 q^2}{m_B}\frac{nE_F}{(E-E_F)^3} + O(\mathbf{q}^4) \quad \text{as } q \to 0 , \qquad (33)$$

it is also easy to see that the magnon dispersion varies, at small q, as $\hbar^2 q^2/2m^*$ with an effective mass m^* equal to $5m_B$. Such a universal relation between the magnon mass and the band mass should not be taken seriously, even within our model, since it results from the special character of the RPA calculation. A more detailed treatment of correlations would lead to the replacement of U in Eq. (28) by a q- and ω-dependent function $U(q,\omega)$ with drastic consequences on the magnon dispersion. As an example, we have considered the finite-range interaction formula

$$U(q) = \frac{U}{1+\gamma(q/k_F)^2} \qquad (34)$$

with $\gamma=1$. This formula is suggested by the fact that in the paramagnetic state $U(q)$ should reduce to the usual function $I(q)$ which is used in microscopic theories[7] of the longitudinal spin susceptibility of the electron gas. The latter can be well approximated by the form of Eq. (34). Further evidence that Eq. (34) might give a good representation of the transverse spin susceptibility has been found by Lowde and Windsor[8] in the analysis of neutron scattering experiments. In Fig. 4 we compare the magnon dispersion for $\gamma=0$ (RPA) and $\gamma=1$. The magnon effective mass is now given by

$$\frac{m_B}{m^*} = \gamma + \tfrac{1}{5} , \qquad (35)$$

so that the magnon energy is considerably enhanced in going from $\gamma=0$ to $\gamma=1$, reaching, in the latter case, a maximum value of $\sim\frac{1}{5}$ of the Fermi energy at the maximum wave vector $q_c=0.5k_F$, beyond which it becomes overdamped. In general, γ can be regarded as an adjustable parameter to fit the observed magnon dispersion.

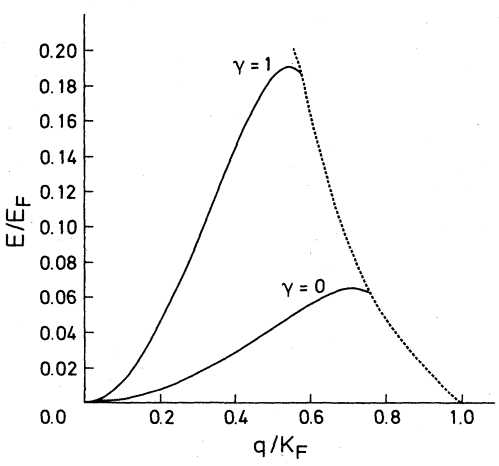

FIG. 4. Magnon dispersion for two values of γ defined in Eq. (34). The dashed line represents the q-dependent Stoner gap $E_-(q)$ of Eq. (32).

Since its actual value does not affect the qualitative features of our discussion, we shall set $\gamma=0$ in the following.

We now turn to the interesting question of the relative weight (integrated cross section) of magnons and Stoner pairs. From Eq. (13) it is easy to see that

$$-\frac{1}{\pi}\int_{-\infty}^{+\infty} dE\, \mathrm{Im}\chi_\sigma(\mathbf{p}_0,\mathbf{q},E) = \frac{1}{Z}\sum_{i,f} e^{-\beta E_i}\langle i \,|\, [\rho_{\sigma,-\sigma}(\mathbf{p}_0,\mathbf{q}),\rho^\dagger_{\sigma,-\sigma}(\mathbf{p}_0,\mathbf{q})] \,|\, i\rangle = \langle \sum_{\mathbf{k}} (n_{\mathbf{k}-\mathbf{q}/2,-\sigma} - n_{\mathbf{k}+\mathbf{q}/2,\sigma})\, V^2(\mathbf{p}_0-\mathbf{k}-\mathbf{q}/2)\rangle . \qquad (36)$$

This exact sum rule represents the generalization of a previously known result for the frequency integral of the transverse spin susceptibility, which states the latter to be equal to $n_\uparrow - n_\downarrow$. It is easy to prove that Eq. (36) is satisfied by our RPA response function since $\mathrm{Im}\chi^{(2)}_\sigma(\mathbf{p}_0,\mathbf{q},E)$ obviously satisfies it, while the second term of Eq. (28) decreases, for large E, as $1/E^2$ and, therefore (from the dispersion relations), does not contribute to the zeroth-moment sum rule. The right-hand side of Eq. (36) can be easily evaluated for our model at $T=0$ with the result

$$-\frac{1}{\pi}\int_{-\infty}^{+\infty} dE\, \mathrm{Im}\chi_\sigma(\mathbf{p}_0,\mathbf{q},E) = \frac{2e^4}{p}\left[\ln\left|\frac{k_F-p}{k_F+p}\right| + \frac{2k_F p}{p^2-k_F^2}\right] , \qquad (37a)$$

where

$$p = |\,\mathbf{p}_0 - \mathbf{q}\,| = (p_0^2 + q^2 - 2\mathbf{p}_0\cdot\mathbf{q})^{1/2} . \qquad (37b)$$

Since $\mathrm{Im}\chi_\sigma(\mathbf{p}_0,\mathbf{q},E)=0$ for $E<0$ when q is less than k_F, Eq. (37a) gives the value of the integrated cross section (for $T=0$) as a function of $\mathbf{p}_0$ and of the momentum transfer $\mathbf{q}$. On the other hand, the contribution of the magnons to the integrated cross section can be directly calculated from Eq. (28) and it is

$$-\frac{1}{\pi}\int_0^\infty dE\, \mathrm{Im}\chi_\downarrow(\mathbf{p}_0,\mathbf{q},E)\,|_{\text{magnons}} = \left|\frac{[\chi^{(1)}_\downarrow(\mathbf{p}_0,\mathbf{q},E_m(q))]^2}{[\partial\chi^{(0)}_\downarrow(q,E)/\partial E]_{E=E_m(q)}}\right| , \qquad (38)$$

where $E_m(q)$ is the energy of the magnon. For large incident momentum, $p_0 \gg k_F$, and small momentum transfer, $q \ll k_F$, both the weights of Eqs. (37) and (38) tend to the common value $V^2(p_0)n$, indicating that the integrated cross section is exhausted by magnons. This is a well-known fact in the theory of neutron scattering from ferromagnetic electrons. At larger q the weight of the pairs increases and that of the magnon decreases so that their sum is given by Eqs. (37). Beyond q_c the weight of the magnon becomes zero. This behavior is shown in the lower part of Fig. 5 for $p_0=10k_F$. Notice that the total

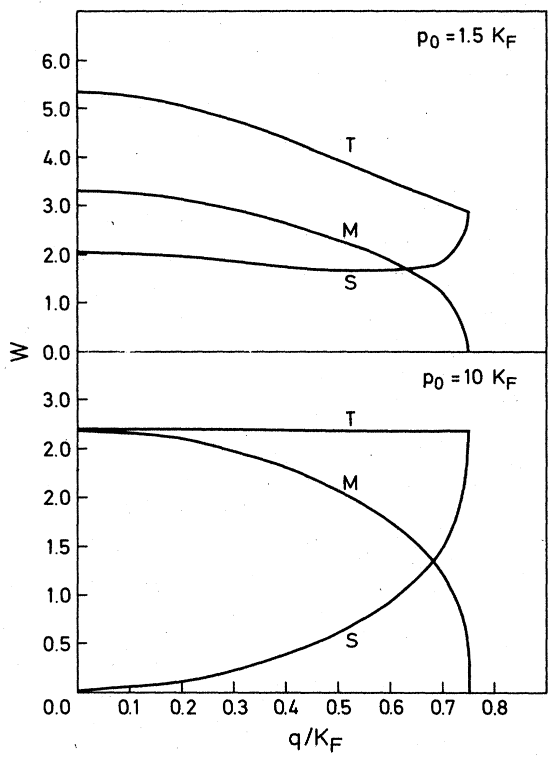

FIG. 5. Integrated cross section (T) and its magnon (M) and Stoner (S) components as functions of q for momentum of the incident electron $p_0=10k_F$ and $p_0=1.5k_F$. The screening wave vector $q_{\rm TF}$ is equal to 0.

weight is almost constant as a function of q. In the upper part of Fig. 5 we consider the case of incident momentum p_0 comparable to k_F, $p_0=1.5k_F$. There are two qualitative differences with respect to the large-p_0 limit. In the first place the Stoner pairs now have a non-negligible weight (about $\frac{2}{5}$ of the total) even in the very-small-q limit. In the second place the total weight is increased and depends more strongly on the value of q. These features are reinforced at smaller values of p_0; for example, at $p_0=1.1k_F$ the Stoner pairs exhaust, in the small-q limit, about $\frac{3}{5}$ of the sum rule. The conclusion is clear; electron-exchange collisions with primary momenta comparable to the band Fermi momentum are an effective probe of the Stoner-pair excitation spectrum for $q\to 0$ and thus of the Stoner gap itself. In contrast to this the neutron scattering technique is mainly a probe for the magnons. The two techniques are, in this respect, complementary to each other.

An unpleasant feature of our RPA calculation is that for p_0 approaching k_F it gives a divergent spectral weight, as can be seen from Eqs. (37). The origin of this divergence is in the lack of screening of the Coulomb potential which puts too much weight on the region of phase space where $\mathbf{p}_0-\mathbf{k}-\mathbf{q}/2$ is minimum. The simplest way to correct this defect is to replace the bare Coulomb interaction by the Thomas-Fermi screened interaction

$$V_{\rm TF}(q)=\frac{4\pi e^2}{q^2+q_{\rm TF}^2}\ , \qquad (39)$$

where $q_{\rm TF}$ is of the order of the Fermi momentum. With this modification Eq. (37a) still holds provided that p is redefined as

$$p=(p_0^2+q_{\rm TF}^2+q^2-2\mathbf{p}_0\cdot\mathbf{q})^{1/2}\ , \qquad (40)$$

and the formulas for $\chi_\sigma^{(1)}(\mathbf{p}_0,\mathbf{q},E)$ are essentially unchanged apart from equally trivial modifications. We have calculated the spectral weights at $p_0=1.5k_F$ for $q_{\rm TF}=k_F$ and we find that the ratio between the magnon and the Stoner contribution is approximately unchanged from the case $q_{\rm TF}=0$; only the total weight becomes smaller and less dependent on q.

Another interesting feature of our calculation appears when we consider the shape of the cross section versus energy loss in the Stoner-pair region. In Fig. 6 we have plotted the corresponding curves for $q=0.2k_F$, $p_0=1.5k_F$ both in the noninteracting ($U=0$) and in the interacting case. The angle between $\mathbf{p}_0$ and $\mathbf{q}$ is taken to be constant and equal to $\cos^{-1}(q/2p_0)$—an approximation which is justified because the energy loss is much smaller than the incident energy. Since we are only interested in the shape of the two curves we normalize both of them to a maximum of 1, although in reality the noninteracting curve has a maximum several times larger than the interacting one. We find that the two curves are indeed very similar; in particular, they both have a peak at about $E=E_F$, which is the value of the exchange splitting. This situation should be contrasted with the corresponding one in the case of neutron scattering. The interacting spin-correlation spectrum in our model has a peak at an energy about 10% smaller than the noninteracting one, which has a peak at E_F. The absence of this "excitonic shift" effect gives further evidence that the electron scattering technique actually probes the single-particle properties of the system.

We conclude our discussion with some remarks about the experimental results of Refs. 1 and 2. A quantitative comparison between theory and experiment is clearly out of question here, since it would require the knowledge of both the spin-flip and the non-spin-flip contributions to

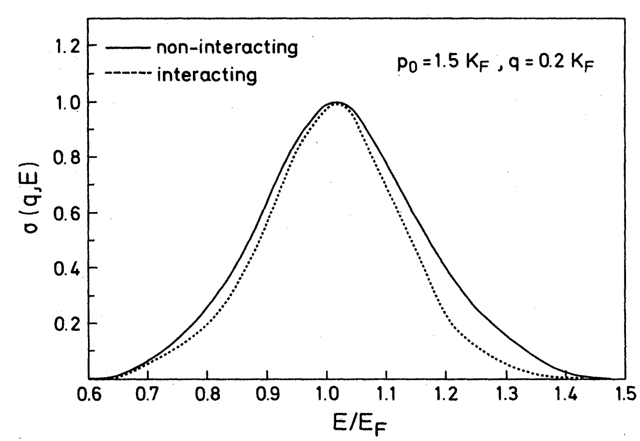

FIG. 6. Differential cross section $\sigma(q,E)$ vs energy loss for the interacting (dashed line) and noninteracting (solid line) system. Both curves are normalized to have a maximum at 1. Notice the coincidence of the two peaks.

the cross section within a realistic model of the band structure. If, however, we limit ourselves to a consideration of the energetic structure of the asymmetry and polarization spectra, we can assume, following Kirschner, Rebenstorff, and Ibach,[2] that they are essentially proportional to the spin-flip cross section. This approximate relationship is due to the fact that the nonflip contributions for incoming electrons of spin ↑ or ↓ are weakly energy dependent in a region around the Stoner gap and their difference is small (see Ref. 2 for details). The constant of proportionality remains, of course, undetermined. This basic limitation should be borne in mind throughout the following discussion. In an electron-energy-loss experiment in which E is much smaller than the initial energy E_0, there are two regimes of interest: the small-angle regime, $\theta \ll E/2E_0$, and the large-angle regime, $\theta \gg E/2E_0$. In the small-angle regime the relation between momentum and energy transfer is

$$q \cong E/\hbar v_0 \ll \hbar k_F \,, \tag{41}$$

where v_0 is the velocity of the incident electron. This is the regime in which the experiment of Ref. 2 is performed. One does not expect to see the magnon here, since the corresponding energy loss would be too small. On the other hand, using Eq. (41), one would expect a very narrow asymmetry spectrum centered around the exchange splitting and with a width

$$\Delta E/E_F \cong 2V_F/V_0 \cong \tfrac{1}{15} \,,$$

if we take $E_0 = 10$ eV, $E_F = 0.3$ eV, and $m_B \cong 30m$ (for Ni). This is clearly in disagreement with the experimental observation of a very broad asymmetry spectrum: $\Delta E/E_F \cong 2$. A very reasonable explanation of this result has already been proposed by the authors of Ref. 2 in terms of the nonuniformity of the exchange splitting over the Brillouin zone. Within our model this would amount to having a k-dependent self-energy correction in Eq. (21). Such a self-energy should come from band structure as well as from many-body effects. Although we have not yet made any quantitative attempt in this direction, it is easy to see that it would indeed give a broadening of the asymmetry spectrum as well as some amount of magnon damping, following from the smearing of the kinematic boundaries for the excitation of Stoner pairs. At larger scattering angle one enters a different regime in which the momentum transfer is decoupled from the energy transfer and it is given by

$$q \cong 2p_0 \sin(\theta/2) \,, \tag{42}$$

or $q \cong p_0\theta$ if $\theta \lesssim 1$. It is not difficult, in this regime, to transfer momenta of the order of the Fermi momentum, and we suggest that it should be possible, in a q-resolved experiment, to observe the magnon peak, if the damping is not too severe.

Finally, we come to the discussion of the energy-loss experiment of Ref. 1. Here, the induced polarization as a function of the energy loss rises rapidly at low energy, has a maximum around the exchange splitting (~ 2.8 eV), and then decreases slowly over a range of several electron volts. The analysis of this result is substantially different from that of the first experiment. The main difference is due to the fact that the target material is now a ferromagnetic iron-based glass which does not exhibit sharp Bragg reflections. The complete scattering process must therefore be pictured as a diffuse elastic reflection from the sample combined with an inelastic process in which some amount of momentum and energy is transferred to the electrons in the sample. Thus, even if the experiment is angle resolved, this does not imply that it is q resolved. On the contrary, a wide range of inelastic momentum transfers can contribute to the scattering in a given direction. It is clear that this spread in momentum will give rise to a spread in energy. In order to reproduce the experimental curve, we integrate the cross section for angles θ from 0° to 90°. In other words we assume that the surface reflects the beam uniformly in all directions and that the inelastic scattering accounts for the amount of momentum which is needed to bring the emerging electron to the direction of observation, which is normal to the sample. The integral over angle is changed in an integral over momentum with the help of Eq. (42). Thus we calculate

$$\sigma(E) = \int_0^{p_0\sqrt{2}} dq\, q\, \mathrm{Im}\,\chi_\sigma(\mathbf{p}_0,\mathbf{q},E)\,|_{\text{Stoner}} \tag{43}$$

over the region of the Stoner pairs, where the angle between $\mathbf{q}$ and $\mathbf{p}_0$ is $\cos^{-1}(q/2p_0)$ and we take the following values of the parameters: $E_0 = 45$ eV, $E_F = 2.7$ eV, $p_0 = 1.3k_F$, $m_B = 10m$, and $V_0/V_F \cong 15$. In Fig. 7 we show the results for the bare interaction model ($q_{\text{TF}} = 0$). The curve has considerable structure. At $E \cong 0.06E_F$, where the magnon merges with the Stoner pairs, it has a first extremely narrow peak; at $E = E_F$ equal to the exchange splitting it has a second and stronger peak; henceforth it decays with a width of about E_F. Introducing the screening ($q_{\text{TF}} = k_F$) tends to round out the structure; in particular, the Stoner peak at $E = E_F$ becomes lower and

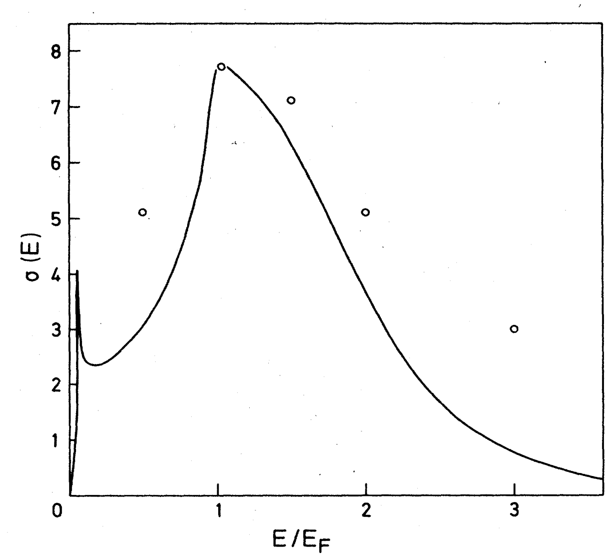

FIG. 7. Inelastic cross section integrated over angles as given in Eq. (43) and discussed in the text. Open circles are taken from Fig. 2 of Ref. 1 rescaled to give the same maximum at $E = E_F$.

broader, but the qualitative behavior remains the same. The Stoner structure in Fig. 7 is in reasonable agreement with that of Fig. 2 of Ref. 1 (open circles) but somewhat narrower. The first peak of Fig. 7, instead, has not been observed, possibly because the resolution was not sufficiently good.

If in Eq. (43) we had used, instead of the response function χ_σ, the transverse spin-spin correlation function appropriate for neutron scattering, we would have found a curve rising sharply at very low frequency reaching a maximum in correspondence of the first peak and then decreasing slowly, with no structure around $E=E_F$. Once more, it appears that neutron scattering is mainly a probe for the collective behavior. Notice, finally, that inclusion of the nonuniformity of the exchange splitting in the analysis of this experiment would lead to a broader curve, in better agreement with the experimental one.

ACKNOWLEDGMENTS

This work was supported in part by the National Science Foundation (NSF) Grant No. DMR-80-11934 and by the Materials Research Center of Northwestern University under a grant from the NSF.

APPENDIX: ANALYTIC EXPRESSIONS FOR $\mathrm{Im}\chi_\sigma^{(1)}(\mathbf{p}_0,\mathbf{q},E)$ AND $\mathrm{Im}\chi_\sigma^{(2)}(\mathbf{p}_0,\mathbf{q},E)$

The imaginary part of the integral in Eq. (27), with $i\omega\to E+i\eta$, can be evaluated in an elementary way for $i=1$ and 2. We first consider the case $\sigma=\downarrow$. We introduce the kinematic boundaries

$$E_\pm(q)=\Delta\pm 2\hbar^2 qk_{F\uparrow}/m_B+\hbar^2q^2/2m_B$$

and

$$E'_\pm(q)=\Delta\pm 2\hbar^2 qk_{F\downarrow}/m_B-\hbar^2q^2/2m_B\ , \tag{A1}$$

where Δ is the exchange splitting equal to the difference of the Fermi energies, $E_{F\uparrow}-E_{F\downarrow}$. Performing the integral we find

$$-\frac{1}{\pi}\,\mathrm{Im}\,\chi^{(2)}(\mathbf{p}_0,\mathbf{q},E)=\frac{2m_Be^4}{\hbar^2 q}\{[F^{(2)}(k_{F\uparrow}^2,\alpha,a,b)-F^{(2)}(k_1^2,\alpha,a,b)]\Theta(E-E_-(q))\Theta(E_+(q)-E)$$
$$-[F^{(2)}(k_{F\downarrow}^2,\alpha',a',b')-F^{(2)}((k_1')^2,\alpha',a',b')]\Theta(E-E'_-(q))\Theta(E'_+(q)-E)\} \tag{A2a}$$

and

$$-\frac{1}{\pi}\,\mathrm{Im}\,\chi^{(1)}(\mathbf{p}_0,\mathbf{q},E)$$
$$=\frac{m_Be^2}{2\pi\hbar^2 q}[F^{(1)}(k_{F\uparrow}^2,k_1^2,\alpha,a,b)\Theta(E-E_-(q))\Theta(E_+(q)-E)-F^{(1)}(k_{F\downarrow}^2,(k_1')^2,\alpha',a',b')\Theta(E-E'_-(q))\Theta(E'_+(q)-E)]\ , \tag{A2b}$$

where

$$F^{(2)}(k^2,\alpha,a,b)=\left[\frac{(2\alpha-b)(2k^2+b)}{4a-b^2}-1\right]\frac{1}{(k^4+bk^2+a)^{1/2}} \tag{A3a}$$

and

$$F^{(1)}(k_1^2,k_2^2,\alpha,a,b)=\ln\left|\frac{2(k_1^4+bk_1^2+a)^{1/2}+2k_1^2+b}{2(k_2^4+bk_2^2+a)^{1/2}+2k_2^2+b}\right|\ . \tag{A3b}$$

The quantities k_1,a,b,α and their primed counterparts are defined as follows:

$$k_1=\frac{m_B}{\hbar^2 q}(E-\Delta-\hbar^2q^2/2m_B)\ ,$$
$$\alpha=k_0^2+q^2+2k_0q\mu_0+2k_1q-2k_0k_1\mu_0\ ,$$
$$a=4k_0^2k_1^2(1-\mu_0^2)+\alpha^2\ ,$$
$$b=2\alpha-4k_0^2(1-\mu_0^2)\ , \tag{A4a}$$

and

$$k_1'=\frac{m_B}{\hbar^2 q}\,|\,E-\Delta+\hbar^2q^2/2m_B\,|\ ,$$
$$\alpha'=k_0^2-2k_0k_1'\mu_0\ ,$$
$$a'=4k_0^2(k_1')^2+(\alpha')^2\ ,$$
$$b'=2\alpha'-4p_0^2(1-\mu_0^2)\ , \tag{A4b}$$

where μ_0 is the cosine of the angle between $\mathbf{p}_0$ and $\mathbf{q}$, and $k_0=p_0$. These formulas are valid for the case of a bare Coulomb interaction. If a screened Thomas-Fermi interaction is used as in Eq. (39), it is easy to see that the above formulas are still valid, with the replacements

$$\alpha\to\alpha+q_{\mathrm{TF}}^2\ ,$$
$$\alpha'\to\alpha'+q_{\mathrm{TF}}^2\ . \tag{A5}$$

Finally, the imaginary part of the functions $\chi_\uparrow^{(i)}(\mathbf{p}_0,\mathbf{q},E)$ are easily obtained from the above formulas by interchanging $k_{F\uparrow}$ with $k_{F\downarrow}$ and replacing Δ by $-\Delta$.

*Present address: Max-Planck-Institut für Festkörperforschung, Heisenbergstrasse 1, D-7000 Stuttgart 80, Federal Republic of Germany.

[1]H. Hopster, R. Raue, and R. Clauberg, Phys. Rev. Lett, **53**, 695 (1984).

[2]J. Kirschner, D. Rebenstorff, and H. Ibach, Phys. Rev. Lett. **53**, 698 (1984).

[3]As discussed by Kirschner, Rebenstorff, and Ibach in Ref. 2, both the polarization and the asymmetry spectra measured in the experiments of Refs. 1 and 2 are approximately proportional to the spin-flip inelastic cross section.

[4]T. Izuyama, D. J. Kim, and R. Kubo, J. Phys. Soc. Jpn. **18**, 1025 (1963).

[5]The condition that the momentum transfer be not too small is dictated by the form of the magnon dispersion which is $\propto q^2$ at small q.

[6]C. S. Wang and J. Callaway, Phys. Rev. B **9**, 4897 (1974).

[7]K. S. Singwi, A. Sjölander, M. P. Tosi, and R. H. Land, Phys. Rev. B **1**, 1044 (1970).

[8]R. D. Lowde and C. G. Windsor, Adv. Phys. **19**, 813 (1970).